

# Panoptic Image Annotation with a Collaborative Assistant

Jasper R.R. Uijlings  
Google Research  
jrrou@google.com

Mykhaylo Andriluka  
Google Research  
mykhayloa@google.com

Vittorio Ferrari  
Google Research  
vittoferrari@google.com

## Abstract

*This paper aims to reduce the time to annotate images for the panoptic segmentation task, which requires annotating segmentation masks and class labels for all object instances and stuff regions. We formulate our approach as a collaborative process between an annotator and an automated assistant agent who take turns to jointly annotate an image using a predefined pool of segments. Actions performed by the annotator serve as a strong contextual signal. The assistant intelligently reacts to this signal by anticipating future actions of the annotator, which it then executes on its own. This reduces the amount of work required by the annotator. Experiments on the COCO panoptic dataset [11, 29, 35] demonstrate that our approach is 17% – 27% faster than the recent machine-assisted interface of [2]. This corresponds to 4× speed-up compared to the traditional manual polygon drawing [49].*

## 1. Introduction

This paper aims to reduce the time it takes to annotate images for the panoptic segmentation task. This requires annotating segmentation masks and class labels for all object instances and stuff regions. Such annotations are expensive: it took 19 minutes for a single image for COCO [11, 35] and 1.5 hours for Cityscapes [17]. In this paper we propose to reduce annotation time by learning to predict how the image should be annotated.

To this end we formulate our approach as a collaborative process between a human annotator and an automated assistant agent who take turns to jointly annotate an image. To see this process in action, Fig. 1a shows an example image and Fig. 1b the current annotation, which is partially machine generated. At this point, the annotator converts one of the *road* segments into *pavement*. The assistant reacts by changing the labels of similar looking segments elsewhere in the image to *pavement* as well. Fig. 1e and 1f show another example image and current annotation. After the annotator corrects the *cup* to be a *bowl*, the assistant adds another *bowl*, as well as a *spoon*, a *bottle*, and a *wooden floor*.

This significantly helps the annotator with its task.

To make this possible, we build on [2]. They proposed to annotate an image by composing segments out of a predefined pool, using an interface in which annotators can repeatedly perform one of the following actions: add a segment from the pool, change the label of a segment, and remove a segment. In this paper we introduce an assistant which can help the annotator by executing some of these actions on its own. Crucially, whenever the annotator performs an action, this immediately provides a ground-truth annotation for a segment. This ground-truth serves as a strong form of context; stronger than the use of *predicted context* in previous works [24, 26, 34, 40, 45, 52]. We propose an automated assistant that reacts intelligently to annotator actions by capitalizing on these strong contextual cues to improve the labeling of other parts of the image.

To summarize, we introduce a framework in which an assistant and an annotator collaboratively annotate an image. The assistant intelligently reacts to annotator input based on context by annotating parts of the image by itself. Experiments on the COCO panoptic dataset [11, 29, 35] demonstrate that our approach is 17% – 27% faster than the recent interface of [2]. This corresponds roughly to 4× faster than traditional manual polygon drawing [49].

## 2. Related Work

**Interactive Segmentation.** Many works address interactive object segmentation. Most classical approaches [3, 5, 8, 46, 18, 15, 21, 41] cast the problem as an energy minimization function defined on a graph which spans over pixels. Many recent methods adapt Fully Convolutional neural networks (FCNs, e.g. [13, 36]) for single object segmentation by using user scribbles or clicks as additional input signal [6, 26, 31, 32, 33, 37, 38, 55]. In [14] they use an FCN to produce pixel-wise embedding space. They combine this with scribbles or clicks and a nearest neighbour classifier to segment objects within video. Polygon-RNN [1, 12] is a recurrent neural net which predicts polygon vertices which an annotator can adjust. In [31] they predict object boundaries using an FCN which accepts boundary clicks, which they turn into an instance using a geodesic path solver [16].

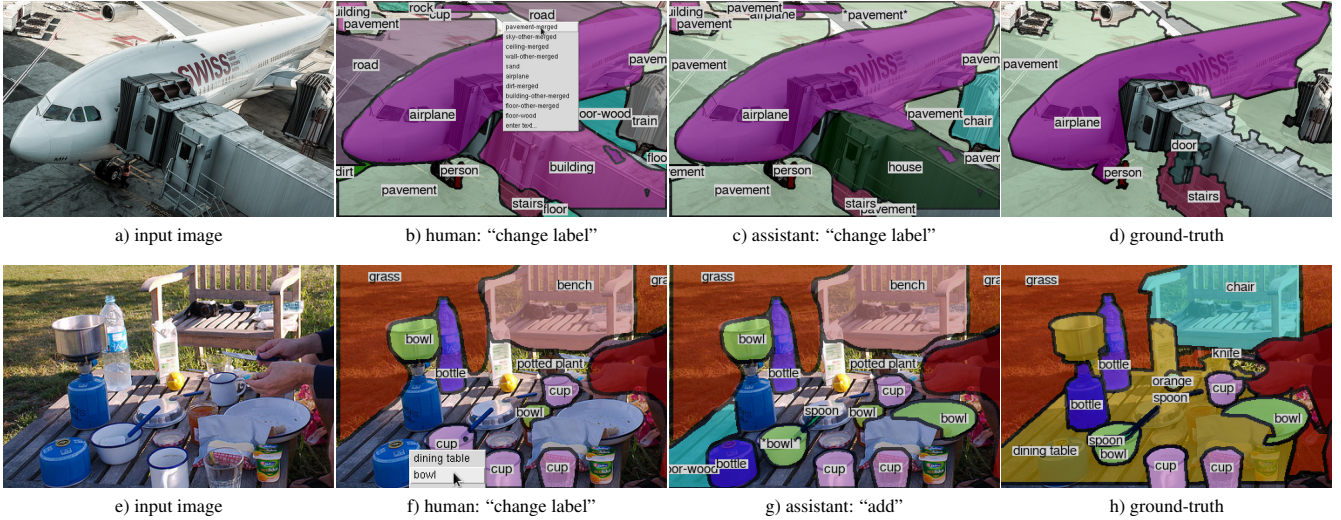


Figure 1. Example of the collaborative annotation process. Given an input image (a), the human annotator and the automated assistant carry out actions in turn. Based on the current annotation, the human performs one action (b) and (f) and then the assistant reacts with a series of actions which it performs on its own (c) and (g). For comparison we show the ground-truth panoptic segmentation in (d) and (h).

The closest related work to ours is Fluid Annotation [2]. Instead of segmenting one object at a time, they propose an interface to quickly annotate a complete image by composing segments out of a pre-defined pool. The interface is designed to facilitate the annotator to perform the action she chooses. In this work we build on top of [2] but go beyond this basic form of assistance: we introduce an assistant that performs some annotation actions on its own.

**Assign annotation tasks.** A few works propose to intelligently choose what annotation task to send to the annotator [30, 53, 48]. In [30] they focus on creating a bounding box for each image-label pair. They have an agent decide whether to ask the annotator to draw a bounding box [42, 51] or verify whether a machine-generated bounding box is good enough [43]. In [48] the machine dispatches annotation tasks to optimize the trade-off between the annotation budget and the final labeling quality. Tasks include providing image labels, providing a label for a certain box, verify a box, draw boxes around other instances of the same class, etc. In [53] they estimate the informativeness and cost of having an image label, a box, or a full segmentation of an image, which they use to dispatch these tasks in an active learning framework. In these works the machine decides which tasks to send to the annotators while the tasks themselves are not interactive. In our case there is a single interface through which both the machine and the annotator interactively take turns.

**Other works on interactive annotation.** In [47] they created a semantic segmentation network which can consume natural language input. This enables a user to correct a machine-predicted segmentation by giving instructions in English. In [9] they propose a framework to convert bounding boxes, instance masks, and part annotations into

each other using human verification and human corrections. Other works address fine-grained classification, where annotators provide feedback or correct the classifiers based on attributes [10, 44, 7, 54].

### 3. Overview

Given an input image we want to produce a dense labelling of every pixel with a semantic label and object identity. This labelling includes both “thing” classes corresponding to various countable objects, and “stuff” classes corresponding to uncountable classes which typically occupy background areas. Example annotations are shown in Fig 1d and 1h.

As a starting point we rely on the recent Fluid Annotation interface [2] that allows to quickly annotate an image by composing segments out of a pre-defined pool (Sec. 3.1). In this paper we turn this into a collaborative environment (Sec. 3.2) and introduce an automated assistant which helps the annotator complete its task (Sec. 4). Crucially, every action of the annotator provides strong contextual cues which the assistant uses to predict how the image should be annotated. Then the assistant *carries out some actions on its own*.

#### 3.1. Fluid Annotation [2]

Fluid Annotation [2] starts by generating a *proposal set* of segments with accompanying class labels using Mask-RCNN [22]. They modified Mask R-CNN to generate about 1000 segments per image, which is more than usual, and to produce segments also on stuff classes (not only on things). The annotator can annotate the image by selecting an ordered subset of these proposals and by optionally correcting their labels. The proposals are ordered to ensure that a

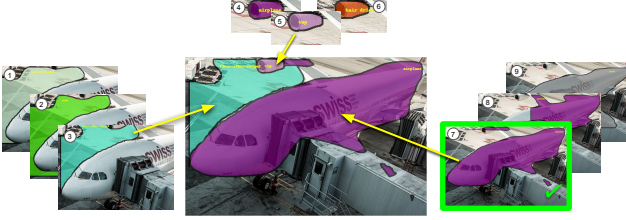


Figure 2. An illustration of the *proposal set*, *active set* and *fixed set*. The *proposal set* is the complete segment pool created by Mask-RCNN (we only show a few segments for clarity). The *active set* defines the current annotation and is composed of segments 3, 5, and 7. The *fixed set* contains segments which were modified by the annotator and are considered to be ground-truth. It consists here of only segment 7. The three sets are nested subsets of each other.

single pixel is assigned to only one segment, following the definition of panoptic segmentation [29].

From the proposal set, the work of [2] first creates an initial annotation for the whole image using an iterative greedy algorithm [2, 29]. Starting from the empty image, first the highest scored segment is selected. Then the next-highest scored segment is placed behind all other segments, if enough of its surface is visible. This greedy algorithm creates an initial ordered *active set*. This active set contains all segments that are currently selected out of the proposal set, and defines the current annotation (Fig. 2). The annotator can modify the active set by performing four kinds of actions: *add a segment* from the proposal set into the active set, *remove a segment*, *change label* of an active segment, and *change depth order* of an active segment. When the annotator completes its job, the active set defines the final annotation.

The Fluid Annotation interface facilitates the actions made by the annotator: when adding a segment, the interface make a small, ordered selection of segments for the annotator to quickly scroll through (based on where the annotator clicked). When changing a label, the interfaces makes a shortlist of likely labels for that segment. Hence in [2] the system facilitates the annotator to perform the action she chose.

### 3.2. Collaborative fluid annotation

In real-world images, different parts are interconnected through contextual relationships. This means that annotating one part of the image will provide a strong signal for how other parts should be annotated. Indeed, Fig. 1 demonstrates that annotating part of the background of the airplane as *pavement* suggests that similar-looking parts should also be labelled as *pavement*. It also demonstrates that annotating a *bowl* suggests that nearby objects are likely to be other types of tableware. This paper capitalizes on this strong contextual signal to extend the influence of each action beyond the one segment targeted by the human annotator.

To that end we extend the Fluid Annotation system with an additional component that we refer to as the *annotation assistant*. This assistant tries to anticipate future actions by the human annotator and automatically executes them. Hence we model annotation as a collaborative environment in which the annotator and the assistant alternate taking actions in turns, both using the same set of actions. Conceptually, the annotator has perfect knowledge about the visual world and about the annotation it aims to achieve. However, it has only partial view of the proposal set, and exploring this set is a costly process. Conversely, the assistant can access all the proposal segments instantly, but has limited capability to judge which proposals belong to the final segmentation the human annotator would like to achieve. The aim of the annotator is to produce a high-quality panoptic annotation. The goal of the assistant is to reduce the overall annotation effort.

Crucially, the annotator conveys his knowledge about the world through every action she takes, essentially creating ground-truth as she goes. This freshly created knowledge provides strong contextual cues which the assistant uses to predict how the rest of the image should be annotated. This enables the assistant to react to the annotator and carry out some actions on its own.

**Fixed Set.** As a way to establish communication between the annotator and the assistant we introduce the notion of a *fixed set*. The fixed set contains all the segments which have been approved by the annotator and therefore is considered to be ground-truth. It is a subset of the active set, which in turn is a subset of the proposal set. An illustration of the *proposal set*, *active set*, and the *fixed set* is given in Fig. 2.

The fixed set is created without any additional costs. Whenever the annotator changes the label of a segment, we know the segment is correct semantically (by construction) and also geometrically (otherwise it would have been better to remove the segment). Whenever the annotator adds a segment, we know it is geometrically correct. Furthermore, if its label is incorrect, then the natural behaviour of the annotator is to correct it immediately afterwards. So we can safely put a newly added segment into the fixed set if the next action of the annotator does not correct its label. This means that segments added by the annotator end up in the fixed set with a delay of one action.

All segments in the fixed set can be considered as ground-truth. Hence the fixed set defines which segments can be used by the assistant as contextual signal to make its predictions. Furthermore, we do not allow the assistant to make changes to the fixed segments since they are already correct.

## 4. Annotation assistant

The assistant and the annotator take turns to collaboratively annotate an image. In our framework, the assistant

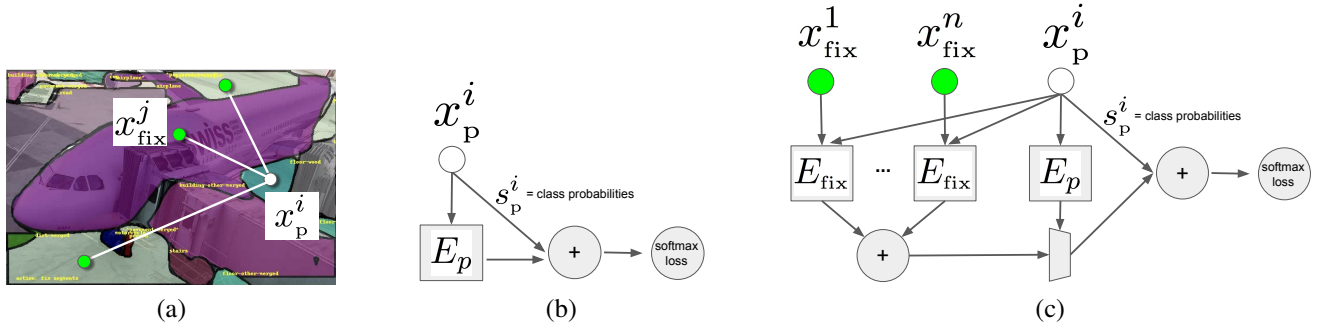


Figure 3. (a) Example image with three fixed segments (green dots), and a proposal segment (white dot). (b) Diagram of a simple model with skip connections that does not have access to fixed segments. (c) Diagram of our context model.

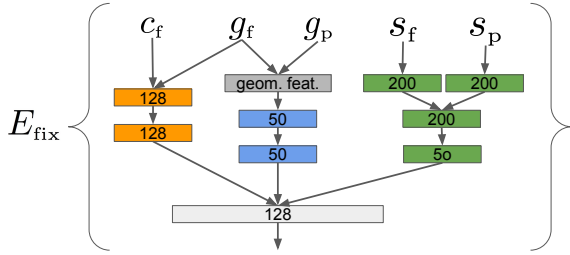


Figure 4. Structure of the  $E_{fix}$  subnetwork. Each of the rectangular blocks corresponds to a fully connected layer with ReLU activation. The number inside each block indicates the number of outputs. The module first independently processes geometric, appearance and human-provided inputs using the layers shown in blue, green and orange respectively and then fuses all inputs together in the final layer (light gray). Note that for simplicity the variable names do not include indices of fixed and proposal segments.

performs as many actions as it wants to, until it decides stop. Then the annotator performs one action. If this action alters the fixed set, the assistant has more information which it can use during its next turn.

We introduce a collaborative assistant in Sec. 4.1. This assistant reacts to context provided by the annotator and can perform the *change label* and *add* actions. We also introduce an initialization agent in Sec. 4.2. It acts before the annotator and replaces the greedy initialization stage of Fluid Annotation (Sec. 3.1).

#### 4.1. Collaborative Assistant (CA)

The objective of our collaborative assistant is to automatically perform actions to accelerate the annotation process. To identify useful actions, this assistant relies on a *context model* that captures dependencies between fixed segments and the segments in the proposal set. In the following we describe the action generation process of the assistant, and then present details of the context model.

**Action generation.** Let us denote the fixed set as  $X_{fix}$ , the class label of a proposal segment  $k$  as  $c_p^k$ , and a binary vari-

able indicating if a segment  $k$  should be present in the active set as  $d_p^k$ . Given initial probabilities for  $c_p^k$  and  $d_p^k$  provided by Mask-RCNN, and all segments in the fixed set, our context model outputs updated probability distributions  $p(c_p^k|X_{fix})$  and  $p(d_p^k|X_{fix})$  for all proposal segments.

The collaborative assistant generates a *change label* action for segment  $k$  when the highest scored label output by the context model is different from the current label. This action updates the label to  $c_p^k = \arg \max_m p(c_p^k = m|X_{fix})$ .

The *add* action is generated when the context model makes  $p(d_p^k|X_{fix})$  greater than a threshold  $\tau$ , and the segment  $k$  is not yet in the active set. In practice we set  $\tau = 0.9$  as estimated on a validation set (Sec. 5).

**Context model.** Let the set of fixed segments be denoted by  $X_{fix} = \{x_{fix}^k | k = 1, \dots, K\}$  and the set of proposal segments by  $X_p = \{x_p^i | i = 1, \dots, N\}$ .

In our model the features of the fixed and proposal segments are given by  $x_{fix}^k = [c_f^k, g_f^k, s_f^k]$  and  $x_p^i = [g_p^i, s_p^i]$  respectively. Each of the variables  $g_f^k$  and  $g_p^i$  corresponds to a 4-dimensional vector encoding the center of the segment and the width and height of its bounding box. The variables  $s_f^k$  and  $s_p^i$  each correspond to a vector of class scores assigned to the segment by Mask-RCNN (one per class in the label space). Finally, the variable  $c_f^k$  denotes a one-hot encoding of the segment class that has been assigned to the fixed segment by the human annotator. Note that the  $c_f^k$  component of the fixed segment representation  $x_{fix}^k$  provides an additional and potentially strong cue for resolving ambiguities in the label of the proposal segments. This is a new piece of information not accessible to Mask-RCNN as usually deployed in computer vision (i.e. without a collaboration with a human).

The structure of our context model is shown in Fig. 3 (c) for the case of the model that updates the class probability distribution  $p(c_p^k|X_{fix})$ . Our starting point for building the context model is a simple update model shown in Fig. 3 (b). This model takes the segment features  $x_p^i$  as input and computes incremental updates to the class probabilities using a fully connected neural network  $E_p$ , similarly to a sin-

gle layer in the ResNet model [23]. We extend this simple model with a sub-network that computes a fixed-size vector summarizing the relationship between the proposal and the fixed set as:

$$\bar{E}_{\text{fix}} = \frac{1}{K} \sum_k E_{\text{fix}}(x_p^i, x_{\text{fix}}^k). \quad (1)$$

The output of  $\bar{E}_{\text{fix}}$  is then combined with the output of  $E_p$  and is passed through a single fully connected layer to compute a difference vector with respect to the original class probabilities of a proposal segment  $x_p^i$ .

We also have second context model, which computes the probability  $p(d_p^k | X_{\text{fix}})$  that segment  $k$  should be present in the active set. This is used by the agent as the basis for the *add* action. This second model has the same structure as the first one (Fig. 3 (c)), with class probabilities  $s_p^i$  replaced by a presence confidence score and the softmax loss replaced by a binary cross-entropy loss (present/absent).

In Fig. 4 we show the structure of the component  $E_{\text{fix}}$  that encodes relationship between a fixed segment and a proposal segment. We follow the late fusion strategy and first apply a series of transformations to each type of input features before finally combining them together. Prior to feeding geometric features  $g_f$  and  $g_p$  into the network, we transform them into a 10-dimensional vector of relative features defined similarly to [25]. Let us denote the offset vector between the locations of the fixed and the proposal segment as  $\Delta_{fp}$ , and after normalization by the width and height of the fixed segment as  $\hat{\Delta}_{fp}$ . The vector of relative geometric features is then obtained by concatenating  $\Delta_{fp}$ ,  $\log(|\hat{\Delta}_{fp}|)$ ,  $\log(w_p/w_f)$ ,  $\log(h_p/h_f)$ ,  $\text{sign}(\Delta_{fp}) \log(|\Delta_{fp}|)$ , and  $\text{sign}(\Delta_{fp}) \log(|\hat{\Delta}_{fp}|)$ .

**Local score pooling.** The model described above can operate with any type of segment scores  $s_p^i$ . We found that instead of directly using the scores provided by Mask-RCNN we achieve higher accuracy by performing a form of max-pooling over the scores of nearby segments. This corresponds to defining a new score vector  $\hat{s}_p^i$  as

$$\hat{s}_{p,c}^i = \max_{j \in N(i,c)} s_{p,c}^j \quad (2)$$

where  $c$  is a class label, and  $N(i, c)$  is the set of segments with label  $c$  that have intersection-over-union  $< 0.5$  with segment  $i$ .

**Training the context model.** The ideal training data for our context model would be composed of training examples derived from the actions performed by real humans during image annotation. Since collection of such training data is impractical we use data collected in simulation. To that end we simulate the fluid annotation process for each of the images in the training set using the simulator described in [2]

and store all segments and their labels contained in the final annotation. To construct training examples of the fixed set for our context model we then randomly sample correct segments out of the final annotation. We found such random sampling to be necessary to make the model robust with respect to the size of the fixed set encountered by the agent when deployed at annotation time. We train the context model using the Adam optimizer [27].

**Discussion.** Our context model has several properties that make it well-suited for use within the annotation assistant. It is flexible with respect to the number of segments in the fixed set, which allows to apply it without modifications at each annotation step. It is also invariant to the ordering in which the segments are added to the fixed set. This is a good property since it is not known in advance which area of the image will be processed first by the human annotator.

A number of previous works attempts to exploit context based purely on image signals [24, 26, 34, 40, 45, 52]. In our paper instead contextual cues are based on *human input*, which makes them much stronger. In terms of technical realization, our context model is related to models used for visual question answering [50] and for modeling relationships between scene objects [25]. Compared to the model of [25] we choose a different approach to utilizing the relational model. While [25] combine weighted appearance vectors of related object detections to recompute class probabilities, we instead use a module similar to relational network in [50] to compute additive updates to class probability vector. Our model is also related to graph convolutional networks [28]. It can be interpreted as a graph convolution based on the Eq. 1 in a rather simple graph in which every proposal segment is connected to every fixed segment, but the proposal segments are not connected to each other.

## 4.2. Initialization Assistant (IA)

In the original Fluid Annotation method, the initialization was done greedily through non-maximum suppression of Mask-RCNN segments based on their scores [2]. In this section we use an initialization assistant to do this instead. The initialization produces a panoptic segmentation by composing segments from the proposal set, without any human annotator involved. This method therefore can also be used for classical image segmentation prediction [13, 29, 36, 39].

We represent each segment as a feature vector consisting of: (a) an 8-bit encoding of the class label predicted by Mask-RCNN; (b) the predicted score of the segment; (c) the percentage of the segment surface that does not overlap with any segments in the current *active set*.

The assistant uses these features to iteratively perform actions, starting from an empty active set. At each time step, it scores all the segments which could be added and select the one with the highest score. If this score is above

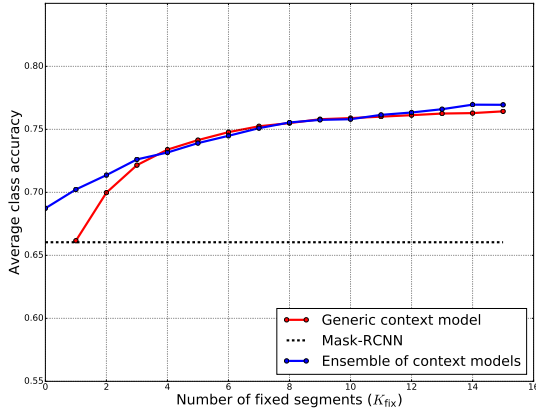


Figure 5. Class label accuracy for varying number of fixed segments obtained by context models trained on COCO-20k .

a certain threshold, it adds the segment to the active set. Otherwise, it stops.

To train our initialization assistant, we collect examples by simulating the full fluid annotation process for each image, similar as in Sec. 4.1. This results in a set of positive *add* actions with their features. To also obtain negative *add* actions, we do a form of hard negative mining. In particular, at several points during the fluid annotation simulation we ask the initialization assistant to make predictions. All predicted *add* actions which are inconsistent with the original ground truth form the negative example set. As model we use a simple 4-layer fully connected neural net. We use a quadratic hinge loss and train using the Adam optimizer [27].

Our initialization assistant is conceptually related to search-based structured prediction (SEARN) algorithm proposed in [19] and other approaches in the literature such as [20, 4] that iteratively generate structured outputs one component at a time. The approach of [4] is particularly close to ours, but addresses a somewhat different task of semantic segmentation and relies on a different feature representation.

## 5. Results

In this section we first evaluate the context model (Sec. 5.1) and then we evaluate the full collaborative annotation process (Sec. 5.2).

**Dataset.** We use the COCO panoptic dataset<sup>1</sup>, which is a combination of the original COCO dataset [35] and COCO-stuff [11], where several stuff classes are merged based on [29]. The dataset contains 120K training and 5K publicly available validation images densely labeled with 80 thing and 53 stuff classes.

We generate two splits of the original training set. We

<sup>1</sup><http://cocodataset.org/index.htm#panoptic-2018>

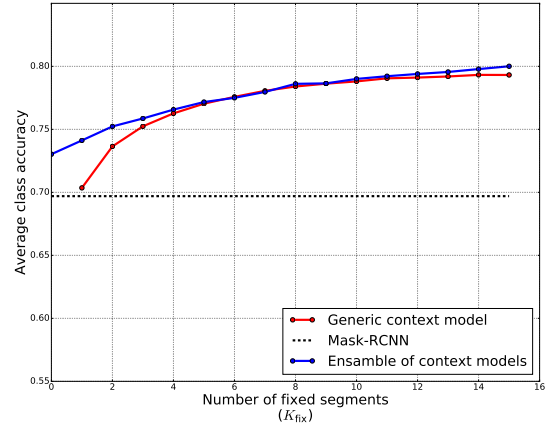


Figure 6. Class label accuracy for varying number of fixed segments obtained by context models trained on COCO-58k .

call the first split COCO-20k . It contains (a) 20K training images which we use to train the Mask-RCNN model that produces the proposal segments; (b) another 20K training images which we use to train our assistant. We call the second split COCO-58k , as it contains 58K images for Mask-RCNN and another 58K for our assistant. We use the validation set of the COCO panoptic dataset for evaluation.

### 5.1. Context model

In this section we evaluate the performance of our context model in isolation. To do this, we want to measure how well the context model can correct labels predicted by Mask-RCNN given a set of fixed segments. However, updating predictions for the whole proposal set does not make much sense; some segments are geometrically wrong while some parts of the image have a disproportionate amount of segments which skews measurements. Hence given an image, the ground-truth and the proposal set, we first approximate each ground-truth segment using one, or in the case of stuff segments, several proposal segments. Let us denote the subset of proposals selected in this approximation as an evaluation set  $E$ . Every proposal in  $E$  is assigned a ground-truth class label equal to the label of the corresponding ground-truth segment. We evaluate the context model given the size of the fixed set  $K_{fix} = |X_{fix}|$  as follows. For each segment  $s \in E$  we generate  $X_{fix}$  by randomly sampling the required number of segments from  $E \setminus \{s\}$  and setting their labels to the ground-truth. We then compare the ground-truth and predicted labels of  $s$  and compute average accuracy by repeating this process for all segments in  $E$ . We consider the accuracy of the segments' class labels as originally assigned by Mask-RCNN as a baseline. Results for a varying number of  $K_{fix}$  are shown in Fig. 5 and Fig. 6 for COCO-20k and COCO-58k respectively.

For the purpose of this evaluation, in addition to a single generic context model we also train a specialized model

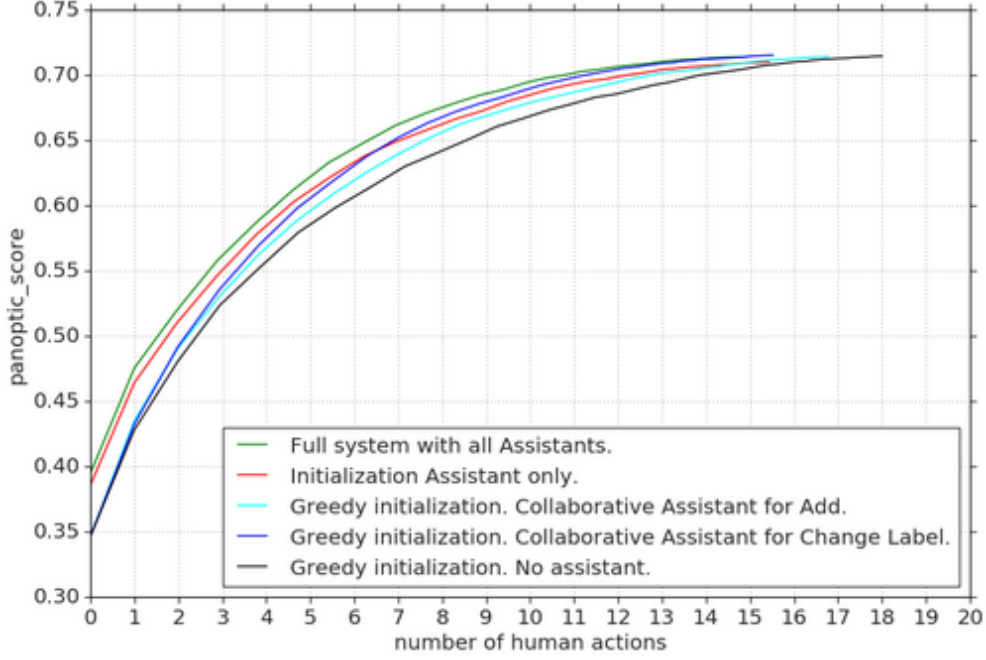


Figure 7. Trade-off between effort and quality for our annotation system. The black line shows the baseline system [2]. The green line is our full system. The other lines are an ablation which evaluates each type of assistance in isolation.

for each value of  $K_{\text{fix}}$ . We refer to a collection of these specialized models as an ensemble model. Overall, both the generic and ensemble context models bring considerable improvements in accuracy over the baseline, and these improvements increase with the size of the fixed set. For example, at  $K_{\text{fix}} = 5$ , the ensemble model trained on COCO-20k improved accuracy from 66% to 73.5%. When training on COCO-58k the trend is similar, but the overall numbers are a bit higher due to the larger training set. In this case, the ensemble model improves from 69% to 77% at  $K_{\text{fix}} = 5$  and further improves to 80% for  $K_{\text{fix}} = 15$ . Note that for  $K_{\text{fix}} = 0$  the accuracy of the ensemble model is higher than the baseline due to local score pooling (see Eq. 2).

Overall we observe that our generic model is able to adapt to the variable size of the fixed set, except for  $K_{\text{fix}} \leq 3$ , where it performs worse than the ensemble model. To address this shortcoming in the experiments in Sec. 5.2 we combine the generic model with three additional models that handle the cases with  $K_{\text{fix}} \leq 3$ .

Based on the results in this section we conclude that the strong context provided by the fixed segments is able to considerably boost classification accuracy. This is greater than what typically demonstrated in classical context works, which do not benefit from conditioning on human input for parts of image [24, 26, 34, 40, 45, 52].

## 5.2. Collaborative annotation process

We now evaluate our assistant in the full collaborative annotation environment. As before, we simulate the annotator, which means she tries to reproduce the original ground-

truth of the COCO panoptic challenge [11, 35]. Having a simulated annotator rather than real humans avoids measuring noise caused by human label disagreement. In this section we use the COCO-58k set for training and evaluate on the COCO validation set. To avoid overfitting, we report results not on the 4500 images used to evaluate the context model, but on the remaining 500 images instead.

Results are presented in Fig. 7, which measures quality (panoptic score [29]) as a function of annotation effort (number of human actions). The black line is the baseline and corresponds to the original Fluid Annotation system [2]: The initialization is done greedily and annotation happens without our assistant. Starting from the greedy initialization, we now introduce two collaborative assistants: one which can only perform the *add segment* action, and another which can only perform the *change label* action. Since they only act after the annotator has performed at least one action, they start from the same point as the greedy initialization. Afterwards, both consistently improve upon the baseline over the full range of the curve. We observe that the effect of the *change label* assistant is the strongest. Intuitively, this makes sense since changing a label of an existing segment is easier than adding a new segment.

The red curve represents initialization done by our initialization assistant (Sec. 4.2). This assistant results in a 4% absolute increase of the panoptic score compared to standard greedy initialization [2, 29]. This suggests that using an assistant is a good way to generate a panoptic segmentation prediction from Mask-RCNN segments, without any humans involved. The good improvement of the initializa-



Figure 8. An example of the annotation process. When the annotator sets a segment to *baseball glove*, the annotator reacts by (1) changing *dirt* to *playingfield* and (2) changing *grass* to *playingfield*.

tion results in a curve which is consistently above the baseline (after initialization there is no further assistance). At around 8 human actions, it is overtaken by the blue curve of the collaborative change label assistant.

To get a better understanding how the assistant reacts, Fig. 8, 9, and 10 shows several examples of the collaborative annotation process of our full system. Notice especially the contextual responses of the assistant: in Fig 8 the *baseball glove* means the background is a *playingfield*, while in Fig. 10 the class *building* means that it is an outdoor scene, prompting the assistant to change *ceiling* to *roof*.

Finally, we combine all agents in our full system: the initialization assistant and the collaboration assistant which performs both *add* and *change label* (green curve). The performance of this full system is better than all other variants. More precisely, the full system only needs 6.2 annotator actions to obtain 0.65 panoptic quality, whereas the baseline [2] requires 8.5 actions, a speed-up of 27%. Similarly, to obtain 0.7 panoptic quality, our full system requires 11.6 annotator actions whereas the baseline requires 14.0 actions, a speed-up of 17%.

Finally, we compare to the cost of manual polygon drawing, which is the most common way to annotate segmen-

tation datasets [17, 35, 39, 56]. The original Fluid Annotation paper reported that their system was  $3\times$  faster than manual polygon drawing (e.g. [49]). Extrapolating, this means that our system is about  $4\times$  faster than manual polygon drawing.

## 6. Conclusions

This paper introduces a framework in which a human annotator and an automated assistant collaboratively annotate an image. The assistant intelligently reacts to annotator input based on context and annotates parts of the image by itself. Results on the COCO panoptic dataset [11, 29, 35] demonstrate that our full system improves annotation efficiency over [2] by 17%-27%. This is about  $4\times$  faster than traditional manual polygon drawing tools (e.g. [49]).

Perhaps the most significant limitation of our context model is that it independently updates each of the proposal segments without considering their mutual relationship. Another limitation is that we capture the relationship between fixed and proposal set at the level of pairwise relationships only, whereas it might be beneficial to consider higher order terms as well. We hope to address both of these limitations in future work.

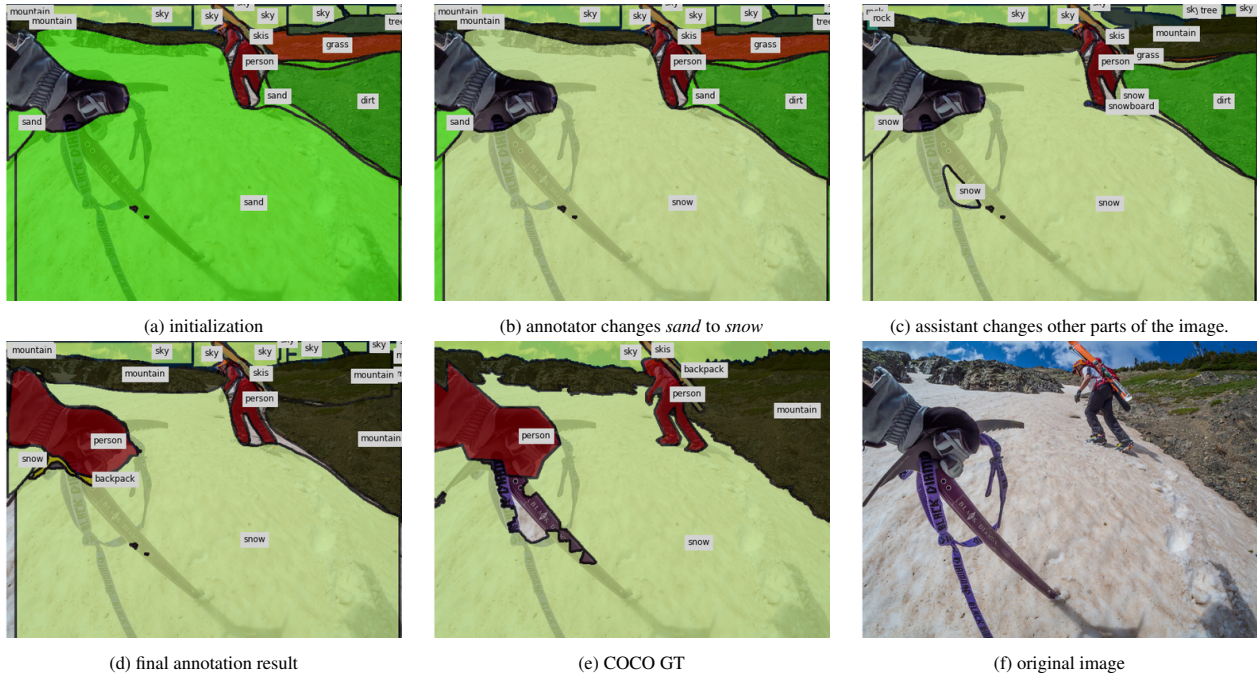


Figure 9. An example of the annotation process. When the annotator changes *sand* to *snow*, the assistant reacts by (1) changing other *sand* segments to *snow*, (2) changing *grass* to the more appropriate *mountain*, and (3) hallucinating a *snowboard* on the shadow of the person, which contextually makes sense.

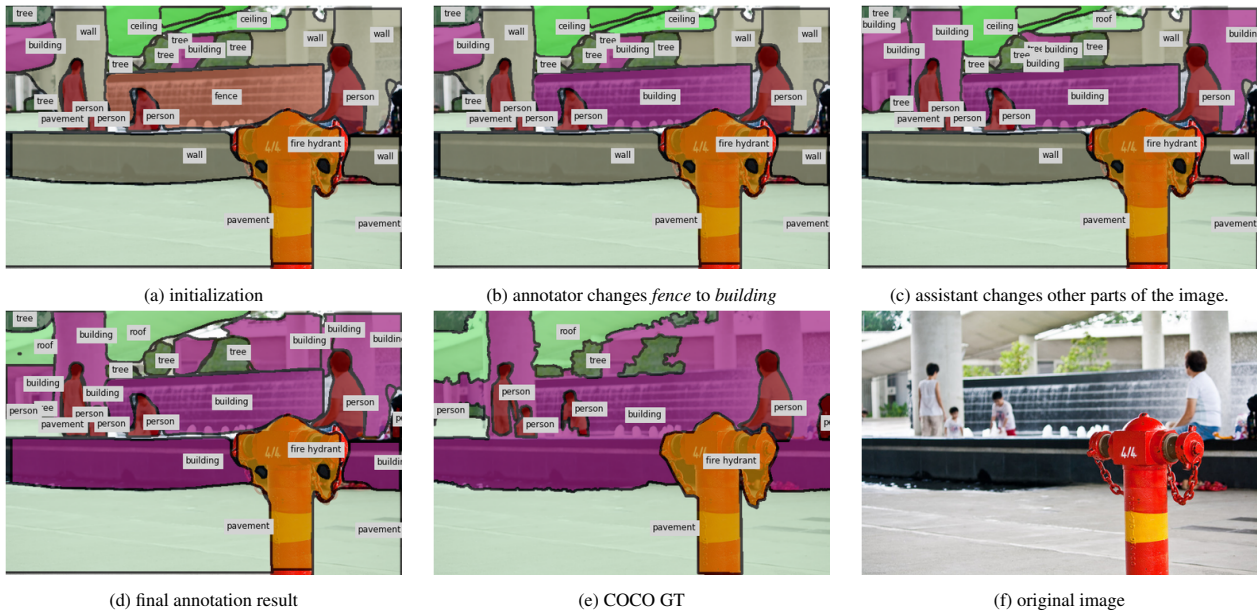


Figure 10. An example of the annotation process. When the annotator changes *fence* to *building*, the assistant reacts by (1) changing several *wall* segments to *building*, (2) adding a *building* segment, and (3) changing one *ceiling* to *roof*, since *building* suggests an outdoor environment.

## References

- [1] D. Acuna, H. Ling, A. Kar, and S. Fidler. Efficient interactive annotation of segmentation datasets with polygon-rnn++. In *CVPR*, 2018. 1
- [2] M. Andriluka, J. R. R. Uijlings, and V. Ferrari. Fluid annotation: A human-machine collaboration interface for full image annotation. In *ACM Multimedia*, 2018. 1, 2, 3, 5, 7, 8
- [3] X. Bai and G. Sapiro. Geodesic matting: A framework for fast interactive image and video segmentation and matting. *IJCV*, 2009. 1
- [4] D. Banica and C. Sminchisescu. Second-order constrained

- parametric proposals and sequential search-based structured prediction for semantic segmentation in rgb-d images. 2015. 6
- [5] D. Batra, A. Kowdle, D. Parikh, J. Luo, and T. Chen. Interactively co-segmenting topically related images with intelligent scribble guidance. *IJCV*, 2011. 1
- [6] R. Benenson, S. Popov, and V. Ferrari. Large-scale interactive object segmentation with human annotators. In *CVPR*, 2019. 1
- [7] A. Biswas and D. Parikh. Simultaneous active learning of classifiers & attributes via relative feedback. In *CVPR*, 2013. 2
- [8] Y. Boykov and M. P. Jolly. Interactive graph cuts for optimal boundary and region segmentation of objects in N-D images. In *ICCV*, 2001. 1
- [9] S. Branson, K. Hjörleifsson, and P. Perona. Active annotation translation. In *CVPR*, 2014. 2
- [10] S. Branson, C. Wah, F. Schroff, B. Babenko, P. Welinder, P. Perona, and S. Belongie. Visual recognition with humans in the loop. In *ECCV*, 2010. 2
- [11] H. Caesar, J. Uijlings, and V. Ferrari. COCO-Stuff: Thing and stuff classes in context. In *CVPR*, 2018. 1, 6, 7, 8
- [12] L. Castrejon, K. Kundu, R. Urtasun, and S. Fidler. Annotating object instances with a Polygon-RNN. In *CVPR*, 2017. 1
- [13] L.-C. Chen, G. Papandreou, I. Kokkinos, K. Murphy, and A. Yuille. Deeplab: Semantic image segmentation with deep convolutional nets, atrous convolution, and fully connected crfs. *IEEE Trans. on PAMI*, 2018. 1, 5
- [14] Y. Chen, J. Pont-Tuset, A. Montes, and L. Van Gool. Blazingly fast video object segmentation with pixel-wise metric learning. In *CVPR*, 2018. 1
- [15] M.-M. Cheng, V. A. Prisacariu, S. Zheng, P. H. S. Torr, and C. Rother. Densecut: Densely connected crfs for realtime grabcut. *Computer Graphics Forum*, 2015. 1
- [16] L. Cohen and R. Kimmel. Global minimum for active contour models: A minimal path approach. In *CVPR*, 1996. 1
- [17] M. Cordts, M. Omran, S. Ramos, T. Rehfeld, M. Enzweiler, R. Benenson, U. Franke, S. Roth, and B. Schiele. The cityscapes dataset for semantic urban scene understanding. In *CVPR*, 2016. 1, 8
- [18] A. Criminisi, T. Sharp, C. Rother, and P. Perez. Geodesic image and video editing. In *ACM Trans. Gr.*, 2010. 1
- [19] H. Daumé III, J. Langford, and D. Marcu. Search-based structured prediction. *Machine Learning*, 75(3):297–325, 2009. 6
- [20] G. Gkioxari, A. Toshev, and N. Jaitly. Chained predictions using convolutional neural networks. 2016. 6
- [21] V. Gulshan, C. Rother, A. Criminisi, A. Blake, and A. Zisserman. Geodesic star convexity for interactive image segmentation. In *CVPR*, 2010. 1
- [22] K. He, G. Gkioxari, P. Dollár, and R. Girshick. Mask R-CNN. In *ICCV*, 2017. 2
- [23] K. He, X. Zhang, S. Ren, and J. Sun. Deep residual learning for image recognition. In *CVPR*, 2016. 5
- [24] G. Heitz and D. Koller. Learning spatial context: Using stuff to find things. In *ECCV*, 2008. 1, 5, 7
- [25] R. Hu, P. Dollár, K. He, T. Darrell, and R. Girshick. Learning to segment every thing. In *CVPR*, 2018. 5
- [26] Y. Hu, A. Soltoggio, R. Lock, and S. Carter. A fully convolutional two-stream fusion network for interactive image segmentation. *Neural Networks*, 2019. 1, 5, 7
- [27] D. P. Kingma and J. L. Ba. Adam: A method for stochastic optimization. In *ICLR*, 2015. 5, 6
- [28] T. N. Kipf and M. Welling. Semi-supervised classification with graph convolutional networks. 2017. 5
- [29] A. Kirillov, K. He, R. Girshick, C. Rother, and P. Dollár. Panoptic segmentation. *arXiv*, arXiv preprint arXiv:1801.00868, 2018. 1, 3, 5, 6, 7, 8
- [30] K. Konyushkova, J. Uijlings, C. Lampert, and V. Ferrari. Learning intelligent dialogs for bounding box annotation. In *CVPR*, 2018. 2
- [31] H. Le, L. Mai, B. Price, S. Cohen, H. Jin, and F. Liu. Interactive boundary prediction for object selection. In *ECCV*, 2018. 1
- [32] Z. Li, Q. Chen, and V. Koltun. Interactive image segmentation with latent diversity. In *CVPR*, 2018. 1
- [33] J. Liew, Y. Wei, W. Xiong, S.-H. Ong, and J. Feng. Regional interactive image segmentation networks. In *ICCV*, 2017. 1
- [34] D. Lin, Y. Ji, D. Lischinski, D. Cohen, and H. Huang. Multi-scale context intertwining for semantic segmentation. In *ECCV*, 2019. 1, 5, 7
- [35] T.-Y. Lin, M. Maire, S. Belongie, J. Hays, P. Perona, D. Ramanan, P. Dollár, and C. Zitnick. Microsoft COCO: Common objects in context. In *ECCV*, 2014. 1, 6, 7, 8
- [36] J. Long, E. Shelhamer, and T. Darrell. Fully convolutional networks for semantic segmentation. In *CVPR*, 2015. 1, 5
- [37] S. Mahadevan, P. Voigtlaender, and B. Leibe. Iteratively trained interactive segmentation. In *BMVC*, 2018. 1
- [38] K.-K. Maninis, S. Caelles, J. Pont-Tuset, and L. Van Gool. Deep extreme cut: From extreme points to object segmentation. In *CVPR*, 2018. 1
- [39] R. Mottaghi, X. Chen, X. Liu, N.-G. Cho, S.-W. Lee, S. Fidler, R. Urtasun, and A. Yuille. The role of context for object detection and semantic segmentation in the wild. In *CVPR*, 2014. 5, 8
- [40] K. Murphy, A. Torralba, and W. T. Freeman. Using the forest to see the trees: A graphical model relating features, objects, and scenes. In *NIPS*, 2003. 1, 5, 7
- [41] N. S. Nagaraja, F. R. Schmidt, and T. Brox. Video segmentation with just a few strokes. In *ICCV*, 2015. 1
- [42] D. P. Papadopoulos, J. R. Uijlings, F. Keller, and V. Ferrari. Extreme clicking for efficient object annotation. In *ICCV*, 2017. 2
- [43] D. P. Papadopoulos, J. R. R. Uijlings, F. Keller, and V. Ferrari. We don't need no bounding-boxes: Training object class detectors using only human verification. In *CVPR*, 2016. 2
- [44] A. Parkash and D. Parikh. Attributes for classifier feedback. In *ECCV*, 2012. 2
- [45] A. Rabinovich, A. Vedaldi, C. Galleguillos, E. Wiewiora, and S. Belongie. Objects in context. In *ICCV*, 2007. 1, 5, 7
- [46] C. Rother, V. Kolmogorov, and A. Blake. Grabcut: Interactive foreground extraction using iterated graph cuts. In *SIGGRAPH*, 2004. 1

- [47] C. Rupprecht, I. Laina, N. Navab, G. D. Hager, and F. Tombari. Guide me: Interacting with deep networks. In *CVPR*, 2018. 2
- [48] O. Russakovsky, L.-J. Li, and L. Fei-Fei. Best of both worlds: human-machine collaboration for object annotation. In *CVPR*, 2015. 2
- [49] B. Russel and A. Torralba. LabelMe: a database and web-based tool for image annotation. *IJCV*, 77(1-3):157–173, 2008. 1, 8
- [50] A. Santoro, D. Raposo, D. G. Barrett, M. Malinowski, R. Pascanu, P. Battaglia, and T. Lillicrap. A simple neural network module for relational reasoning. In *NIPS*. 2017. 5
- [51] H. Su, J. Deng, and L. Fei-Fei. Crowdsourcing annotations for visual object detection. In *AAAI Human Computation Workshop*, 2012. 2
- [52] J. Tighe and S. Lazebnik. Understanding scenes on many levels. In *ICCV*, 2011. 1, 5, 7
- [53] S. Vijayanarasimhan and K. Grauman. What’s it going to cost you?: Predicting effort vs. informativeness for multi-label image annotations. In *CVPR*, 2009. 2
- [54] C. Wah, G. Van Horn, S. Branson, S. Maji, P. Perona, and S. Belongie. Similarity comparisons for interactive fine-grained categorization. In *CVPR*, 2014. 2
- [55] N. Xu, B. Price, S. Cohen, J. Yang, and T. Huang. Deep interactive object selection. In *CVPR*, 2016. 1
- [56] B. Zhou, H. Zhao, X. Puig, S. Fidler, A. Barriuso, and A. Torralba. Scene parsing through ADE20K dataset. In *CVPR*, 2017. 8